J Appl Electrochem (2010) 40:739–747
DOI 10.1007/s10800-009-0052-7

ORIGINAL PAPER

Corrosion protection of mild steel by polyvinylsilsesquioxanes coatings in 3% NaCl solution

A. M. Fekry · Adlia A. A. Gasser · M. A. Ameer

Received: 11 May 2009 / Accepted: 1 December 2009 / Published online: 18 December 2009

Abstract Polyvinylsilsesquioxanes (PVS) coatings were synthesized by the hydrolytic polycondensation of vinyltrimethoxysilane using hydrochloric acid as a catalyst. Their structure was characterized by Fourier transform IR (FTIR) and the viscosity [in centipoise(cP)] of polyvinylsilsesquioxanes was measured at 298 K. The electrochemical behavior of I–IV coated steel electrodes, of polymer concentration as follows: [I(20%), II(40%) of viscosity 50 cP and III(20%), IV(40%) of viscosity 15 cP], was investigated in 3% NaCl solution using various electrochemical techniques, i.e., open-circuit potential (OCP), potentiodynamic polarization, electrochemical impedance measurements (EIS), and surface examination via scanning electron microscope (SEM) technique. The influence of immersion time on the electroctrochemical behavior of polysilsesquioxane-coated electrodes was also studied. The results of polarization measurements showed that corrosion current density (i_{corr}) decreases in the order IV > III > II > I. Also, the film resistance is the highest for PVS-coated electrode I as evaluated from EIS measurements. OCP, EIS, and polarization results are in good agreement with each other. The obtained results were confirmed by surface examination using scanning electron microscope.

Keywords Steel · Polyvinylsilsesquioxanes · Coating · EIS · SEM

A. M. Fekry (✉) · M. A. Ameer
Chemistry Department, Faculty of Science, Cairo University, Giza 12613, Egypt
e-mail: hham4@hotmail.com

M. A. Ameer
e-mail: mameer_eg@yahoo.com

A. A. A. Gasser
Egyptian Petroleum Research Institute (EPRI), Nasr City, Cairo, Egypt

1 Introduction

Conducting polymer films are used for various applications: electro chromic devices [1], photoelectrochemical devices [2], rechargeable batteries [3], sensors [4, 5], and corrosion protection [6–9]; frequently involve structural modification of the polymer backbone to enhance the properties, e.g., incorporation of various functional groups changes conductivity and porosity. Polysilsesquioxanes with a formula of $(RSiO_{3/2})_n$ are increasingly being considered as an alternative to siloxane in applications where high strength, thermal stability, or chemical resistance is a premium [10, 11]. Polysilsesquioxanes used as coatings [12–15] are commonly synthesized through preparing prepolymers based on acid-catalyzed hydrolysis and condensation of organotrialkoxysilanes or organotrichlorosilanes. The hydrolysis of alkoxysilanes leads to the formation of silanol. Their condensation with each other or with alkoxysilanes results in the production of siloxanes. Chemically, the hydrolysis process can be represented as the following reactions:

$$\equiv \text{Si-OR} + \text{H}_2\text{O} \rightleftharpoons \equiv \text{Si-OH} + \text{ROH}$$
$$\equiv \text{Si-OR} + \text{HO-Si} \equiv \rightleftharpoons \equiv \text{Si-O-Si} \equiv + \text{ROH}$$
$$\equiv \text{Si-OH} + \text{HO-Si} \equiv \rightleftharpoons \equiv \text{Si-O-Si} \equiv + \text{H}_2\text{O}$$

Polydimethylsiloxane has no spinnability and no film formation which limit using it as a material for fibers and thin films. Polysilsesquioxanes having such properties together with the chemical, physical, and mechanical properties similar to the silicone are conveniently obtained by sol–gel method. Polysilsesquioxanes are a potential candidate for novel high performance coatings, because they show an appreciable stability to self-condensation, spinnability, and film formation [16]. Abe et al. [14] found that the adhesion and hardness of polyvinylsilsesquioxane coating films, regardless of the substrates,

increased with increasing heating time and moreover molecular weight of polyvinylsilsesquioxane.

Polyvinylsilsesquioxanes (PVS) with very low viscosity were synthesized via the sol–gel process of vinyltrimethoxysilane using hydrochloric acid as a catalyst. An environmentally friendly polyvinylsilsesquioxanes coating films on steels with good adhesion and hardness were obtained. They are environmentally friendly due to of their thermal stabilities and flame-retardant properties. The aim of this work is to study the electrochemical behavior of polyvinylsilsesquioxanes-coated steel and its corrosion properties.

2 Experimental

2.1 Preparation of polyvinylsilsesquioxanes

Into a four-necked flask equipped with a stirrer, a nitrogen inlet, and outlet tubes, a mixture of vinyltrimethoxysilane (VTS 12.35 g, 0.085 mol) and methanol (7 mL) were placed [14] and then cooled in an ice bath for 10 min. An aqueous hydrochloric acid solution was added drop by drop in the molar ratios of r_1 (H_2O/VTS) = 0.86 and 1.04 and r_2 (HCl/VTS) = 0.041 and 0.051 using a 1 M HCl solution. The mixture was stirred at room temperature for 10 min, followed by stirring at 343 K for 3 h under a regulated nitrogen flow. Solvent was removed under reduced pressure to provide viscous liquids of polyvinylsilsesquioxanes.

2.2 Viscosity measurements

The viscosity (in centipoise) of polyvinylsilsesquioxanes obtained was measured at 298 K with Brookfield Digital Rheometer Model DV-III.

2.3 Characterization

Polyvinylsilsesquioxanes were identified using Perkin-Elmer instrument, spectrum one, Fourier transform, IR spectrometer (disc method).

2.4 Preparation of polyvinylsilsesquioxanes films

The steels substrates were polished with emery papers and then washed with water, acetone, and dried in air. The substrates were dipped into 40 wt% and 20 wt% acetone/methanol (w/w = 1) polyvinylsilsesquioxanes solution and then pulled up and this process was repeated two times. The coating films thus obtained were dried at 353 K for 2 h before characterization.

2.5 Electrochemical experiments

The composition of the steel is as follows: C = 0.31, Si = 0.21, Mn = 0.81, P = 0.014, S = 0.017, Cu = 0.06, Cr = 0.02, Mo = 0.01, Ni = 0.02, Sn = 0.0, V = 0.002. The test electrolytes were prepared using sodium chloride (Analar grade reagent) with triple distilled water. OCP, EIS, and potentiodynamic measurements were carried out using the electrochemical workstation IM6e Zahner-elektrik GmbH, MeBtechnik, Kronach, Germany provided with Thales software. The experiments were always carried in an air thermostat which was kept at 298 K.

2.6 SEM observation

The electron microscope used is JEOL-JEM-100 s type with magnification of 100x.

3 Results and discussion

In our work two samples of polyvinylsilsesquioxanes oligomers were prepared by the partial hydrolysis and condensation of vinyltrimethoxysilane in the presence of hydrochloric acid in methanol. According to Eq. 1, data in (Table 1) summarizes the viscosities (in centipoise) at 298 K of polyvinylsilsesquioxanes obtained

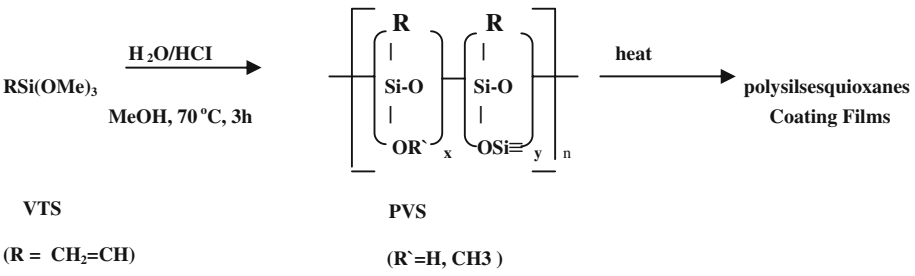

1

Table 1 Viscosity measurement of polyvinylsilsesquioxane formed by hydrolysis

Ex. no.	Molar ratio [r_1(H_2O/VTS)]	Molar ratio [r_2(HCl/VTS)]	Viscosity at 25 °C (cP)	Concentration (%)
I	1.04	0.051	50	20
II	1.04	0.051	50	40
III	0.86	0.041	15	20
IV	0.86	0.041	15	40

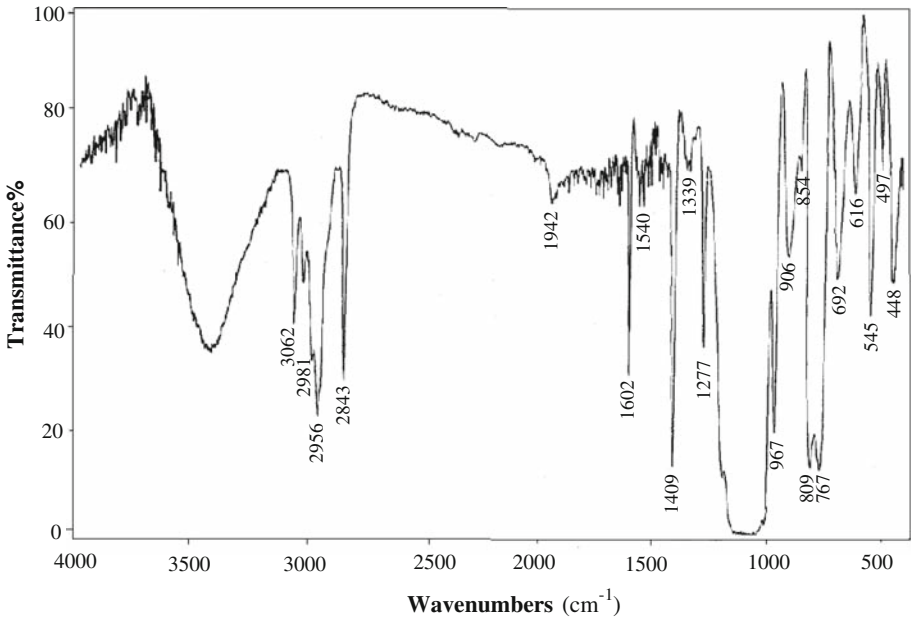

Fig. 1 IR spectra of polyvinylsilsesquioxane (hydrolysis condition of vinyltrimethoxysilane: r_1 (H_2O/VTS) = 1.04; r_2 (HCl/VTS) = 0.051; MeOH = 7 mL; reaction temperature = 70 °C and reaction time = 3 h)

Figure 1 shows the FTIR spectra of polyvinylsilsesquioxanes. The peak intensities due to methoxy group at 2850 cm^{-1} and at 3400–3500 cm^{-1} due to silanol group are observed [17]. Also, the appearance of peak at 1130 cm^{-1} and peaks at 1600, 1400 and 1000 cm^{-1} can be referred to presence of siloxanes and double bond, respectively [18], which clearly indicates that the hydrolysis and condensation proceeded to form polyvinylsilsesquioxane.

3.1 Open circuit measurements

The open-circuit potential (OCP) of PVS-coated electrodes (I–IV) was measured and referred relative to saturated calomel electrode (SCE). Polysilsesquioxane-coated steel electrodes preparation gives always a fixed exposed surface area of 0.47 cm^2. Measurements were collected as a function of the exposure time within a period of 74 h following immersion of the coupons in naturally aerated 3% NaCl solution at 298 K as shown in Fig. 2. It is noticed that the potential shifts to negative values with time for I–III PVS-coated electrodes, it decrease slightly at first few hours (~6 h) then it becomes steady-state value, this may be due to dissolution [19]. In case of PVS-coated electrode IV, the open circuit potential decreased sharply towards more negative values in the first day then it becomes steady-state value. However, the order of E_{ss} value (steady state potential) for the PVS-coated electrodes is IV < III < II < I, where IV has the most negative E_{ss} value where the polymer concentration is 40% acetone/methanol (w/w = 1) polyvinylsilsesquioxanes solution and its viscosity is 15 cP. It seems that film IV protection

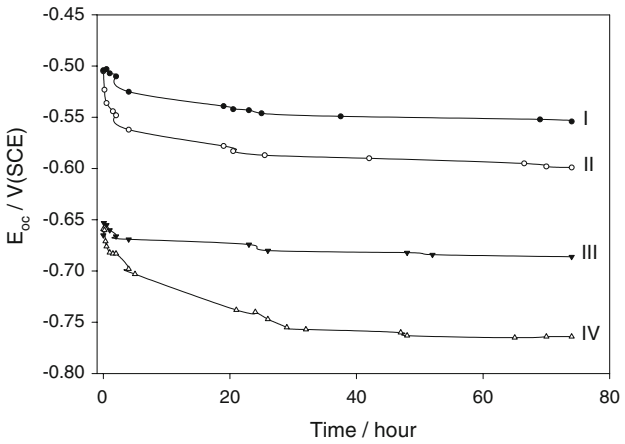

Fig. 2 OCP of I–IV coated electrodes with time in 3% NaCl solution at 298 K

performance is poor due to easy penetration of chloride ions on steel surfaces [19]. It has been observed that the film dissolves quickly in the first day such that the solution becomes yellow, then orange, and after 3 days, the alloy surface becomes black, then the film drops in the solution. However, for the other films (II and III), the solution becomes yellow after 2 days except for the film formed on electrode I, it dissolute at the third day, and for the three films (I–III) the surface becomes reddish brown in color at the third day. So, polysilsesquioxane-coated electrode I shows much better corrosion protection than other films where its polymer concentration is the lowest (20%) and its viscosity is the highest (50 cP). This is due to the resistance of its coating against penetration of corrosive chloride anions. Also, this coating begins to loose protective properties with increasing immersion time due to the fact that easy penetration of corrosive chloride ions [19] on electrode surface is not hindered.

3.2 Potentiodynamic polarization measurements

Potentiodynamic polarization analyses were performed to assess the corrosion performance of the PVS-coated electrodes. A conventional three-electrode cell was used with working electrode as mild steel, saturated calomel electrode as reference, and auxiliary coiled platinum wire as counter electrode for polarization experiments. All samples were immersed in 3% NaCl solution for 74 h before testing at 298 K. Potentiodynamic measurements were performed within the range from −1000 to −200 mV versus SCE at a scan rate of 1 mV/s. Figure 3 shows a typical linear sweep potentiodynamic traces for PVS-coated electrodes in 3% NaCl solution. Both the cathodic and anodic curves exhibit Tafel behavior. These results enable the determination of various electrochemical corrosion parameters of the two

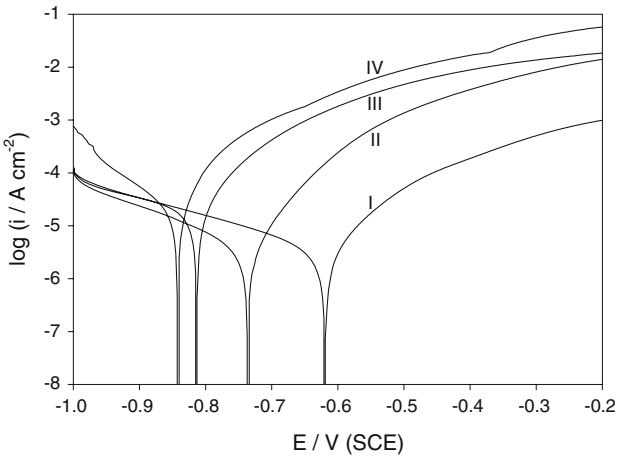

Fig. 3 Potentiodynamic polarization of I–IV coated electrodes with time in 3% NaCl solution at 298 K

Table 2 Data for the polarization of polyvinylsilsesquioxanes-coated electrodes

	i_{corr} (μA cm^{-2})	E_{corr} (mV)	β_a (mV dec^{-1})	β_c (mV dec^{-1})
I	2.1	−625	63.9	−94.0
II	2.4	−732	65.0	−91.5
III	5.5	−816	62.5	−99.1
IV	6.3	−847	64.3	−93.1

electrodes using Thales software for *i*/*E* analysis [20–22]. To avoid the presence of some degree of nonlinearity in the Tafel slope region of the obtained polarization curves, the Tafel constants were calculated as the slope of the points after E_{corr} by 50 mV using a computer least squares analysis. The corrosion current was then determined by the intersection of the cathodic or the anodic Tafel line with the OCP [23] (potential of zero current in the potentiodynamic curves or E_{corr}). This point determines the potential (E_{corr}) and current density (i_{corr}) for corrosion.

For all tested PVS-coated electrodes, the active dissolution parameters were estimated and given in Table 2 as a function of film type (I–IV). The values of the corrosion parameters, corrosion potential (E_{corr}), corrosion current density (i_{corr}), Tafel slopes (β_a and β_c) were calculated and presented in Table 2. The cathodic polarization curves are similar in nature, indicating that same cathodic reaction occurs at the surface of PVS-coated electrodes with different rates for each film concentration.

The results indicate clearly that E_{corr} increases negatively with the increase of corrosion current density (i_{corr}) that is the corrosion rate decreases in the same order as in OCP results IV > III > II > I. It could be seen that PVS-coated electrode I has the highest anticorrosion property and IV has higher rate of dissolution which is in a good agreement with OCP measurements. Also all films form dark black film on the electrode surface after polarization and the solution turns brownish orange color.

3.3 EIS measurements

A conventional three-electrode cell was used with rectangular platinum sheet as counter electrode for impedance measurements. For the impedance experiments, the excitation ac signal has an amplitude of 10 mV peak to peak in a frequency domain from 0.1 Hz to 100 kHz. Electrochemical impedance experiments of coated electrodes were measured in naturally aerated 3% NaCl solution with immersion time (74 h). Impedance measurements provide information on both the resistive and capacitive behavior of the interface and make possible to investigate the performance of a polymer coating as a protective layer against metal corrosion [24]. The experimental EIS diagrams

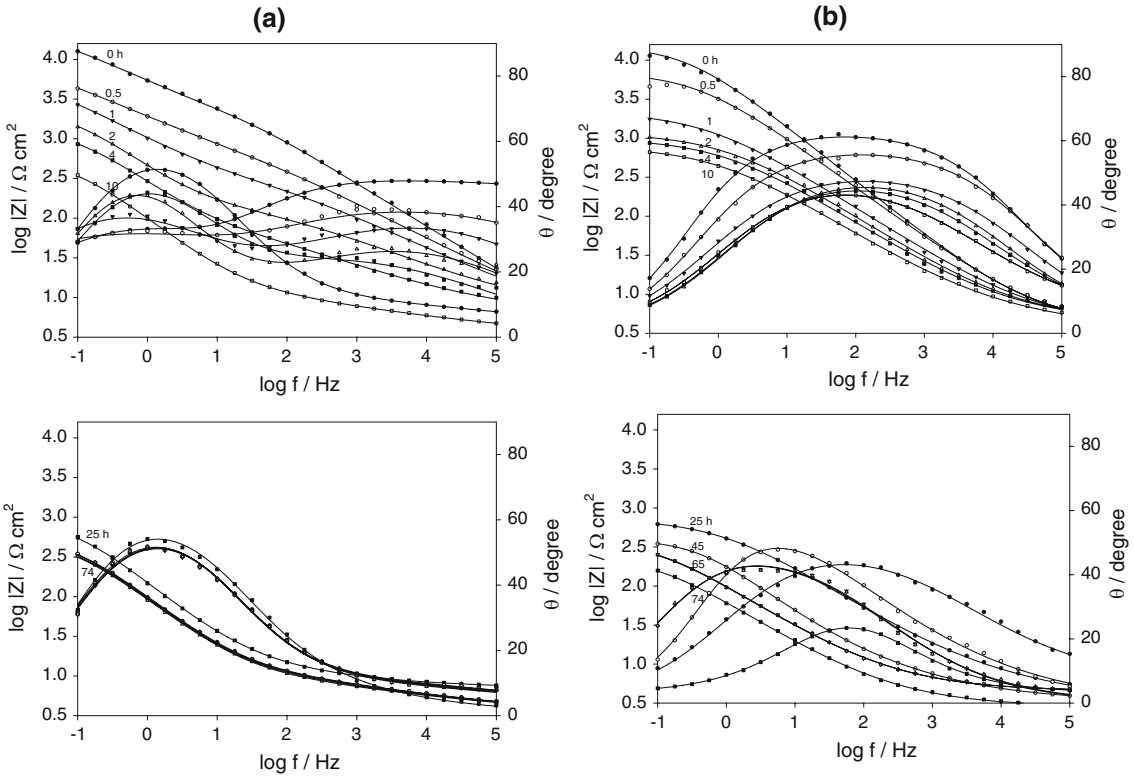

Fig. 4 Bode plots of **a** I and **b** II coated electrodes with time in 3% NaCl solution at 298 K

(Bode plots) are displayed in Fig. 4a, b, as an example, for coated-mild steel I and II, respectively. The impedance (|*Z*|) as well as the phase shift (θ) of mild steel alloy are clearly found to depend on both nature of coating polymer and immersion time. The results in general reveal two clear trends concerning the number of peaks observed in the patterns of the phase shift. The first one is for the behavior of film formed on PVS-coated electrode IV at all times of immersion (0–74 h) and coated electrode II, III at times of immersion from 25 to 74 h, where the Bode plots display only one maximum phase lag. The second trend is for coated electrode I at all times of immersion and coated electrode II, III at times of immersion from 0 to 10 h, where another peak of phase lag appears at the low frequency region or a large phase peak appears could be indicative of the interaction of at least two time constants [25]. However, for coated electrode I and II at times of immersion from 0 to 10 h, there is a diffusion phenomenon.

Computer simulation of the EIS results was performed using a complex nonlinear least-square (CNLS) fitting procedure in order to establish which electrical equivalent circuit (EEC) best fits the experimentally obtained impedance data. The impedance data were thus simulated to the appropriate equivalent circuit for the cases with one time constant (Fig. 5a) and the others exhibiting two time constants (Fig. 5b, c), respectively. This is the simulation that gave a reasonable fit using the minimum amount of circuit components. Generally, the impedance response of an actively corroding metal in an aqueous solution is well simulated by the classic parallel resistor capacitor (RC) combination in series with the solution resistance (R_s) between the specimen and the reference electrode. In this model a charge transfer resistance (R_t) is in parallel with the double layer capacitance (C) which is not ideal and called constant phase element (CPE) for the double layer capacitance, as depicted in Fig. 5a [23]. On the other hand, a two-time constant circuit model with five-element RC was proposed to simulate the metal/film/solution interface as shown in Fig. 5b, c. Figure 5b is a model which consists of two circuits in series from $R_{t1}CPE_1$ and $R_{t2}CPE_2$ parallel combination and the two are in series with R_s. In this way CPE_1 is related to contribution from the capacitance of the outer layer and the faradaic reaction therein and CPE_2 pertains to the inner layer, while R_{t1} and R_{t2} are the respective charge transfer resistances of the outer and inner layers constituting the surface film, respectively [26, 27]. Figure 5c is the same model as shown in Fig. 5b but a Warburg type impedance (Z_w) is inserted to account for diffusion process. Analysis of the experimental spectra were made by best fitting to the corresponding equivalent circuit using Thales software provided with the workstation

where the dispersion formula suitable to each model was used [26, 27]. In this complex formula an empirical exponent (α) varying between 0 and 1, is introduced to account for the deviation from the ideal capacitive behavior due to surface inhomogeneities, roughness factors, and adsorption effects. An ideal capacitor corresponds with $\alpha = 1$ while $\alpha = 0.5$ becomes the CPE in a Warburg component [28]. The presence of an almost potential independent time constant is noticed at lower frequencies, with phase angle close to 45°, corresponding to the diffusion control in the coated layer. This result corroborates the use of the Warburg component [29]. In all cases, good conformity between theoretical and experimental was obtained for the whole frequency range with an average error of 5%. The experimental values are correlated to the theoretical impedance parameters of the equivalent model given in Table 3a–d. CPE can also be related to static disorders such as porosity and may include contribution from dynamic disorders such as diffusion [30]. The impedance associated with the capacitances of the oxide layers is described by the complex frequency dependent impedance (Z_{CPE}) defined as [23, 26, 27]:

$$Z_{CPE} = \frac{1}{C(j\omega)^{\alpha}} \tag{2}$$

where C is the frequency-independent real constant of the CPE, ω being the angular frequency ($\omega = 2\pi f$) in rad s^{-1}, f is the frequency and j is $\sqrt{-1}$, α being the exponent of CPE, with values between -1 for a perfect inductor and 1 for a perfect capacitor. A value of α is associated with the non-uniform distribution of current as a result of roughness and surface defects [23].

The resulting parameters from best fitting of experimental EIS data were presented in Table 3a–d, since the passive oxide film can be considered as a dielectric plate capacitor, the passive film thickness (d) in cm is related to the capacitance (C) by the equation [31]

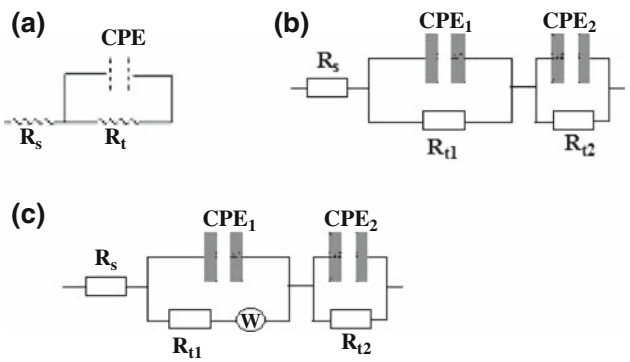

Fig. 5 Equivalent circuits model representing impedance behavior of **a** one, and **b**, **c** two time constants for an electrode/electrolyte solution interface

$$d = \varepsilon_0 \varepsilon_r A / C \tag{3}$$

where ε_o is the vacuum permittivity (8.85×10^{-12} F cm^{-1}), ε_r is the relative dielectric constant of the film and A is the electrode area in cm^2. Although the actual value of ε_r within the film is difficult to estimate, a change of C can be used as an indicator for change in the film thickness [32]. Hence, the reciprocal capacitance ($1/C$) of the surface film is directly proportional to its thickness [33, 34].

The impedance parameters of PVS-coated electrodes (I–IV) are summarized in Table 3a–d. Most authors agree that the equivalent circuits shown in Fig. 5a–c can be used for analysis of impedance data for polymer coated metals which have been exposed to corrosive media [35, 36]. For all coated electrodes, the charge transfer resistance, R_t, describes the resistance of a coating to the penetration of water or electrolyte, which is frequently used to evaluate anticorrosive property of the coated electrode [37]. Also, R_t, provides information concerning degradation of the protective properties of the coating [35, 36]. From the data, it was clearly seen that the resistance of the coated electrodes decreases during exposure time of 74 h. This decrease is due to a decrease in the electronic and ionic resistance of the polymer and replacement of the counter ions in solution with chloride ions in polymer, resulting in increased capacitance. The changes of the coating capacitance with exposure time can be used to determine the water up-take of the coating. For coated electrode I and II at times of immersion from 0 to 10 h in NaCl medium fitted to model shown in Fig. 5b, Warburg behavior in low frequency region was observed (Fig. 4a, b), which indicates the resistive of the coating against the diffusion of the corrosive ions in the coated electrode [19].

R_t and CPE jointly belong to the electrochemistry of corrosion at the polymer–metal interphase after coating penetration by corrosive anions [19]. Figure 6a shows a pronounced increase in CPE_T (total capacitance) for the coated electrodes in the order of IV > III > II > I. Also, R_T (total resistance) decreases with immersion time as shown in Fig. 6b. So, the results indicate that the viscosity is more effective than the concentration of PVS-coatings. So, for PVS-coated electrode I, it could still provide anticorrosion performance very well after 74 h immersion, further indicating that film I coatings had better corrosion resistance [38].

3.4 Morphologies and surface characterization of polysilsesquioxane films

The results were confirmed using surface examination. All corroded specimens were rinsed gently with distilled water, dried, and stored in a desiccator for several days

Table 3 Impedance parameters for (a) I, (b) II, (c) III, and (d) IV polyvinylsilsesquioxanes-coated electrodes after 74 h immersion in 3% NaCl solution at 298 K

Time (h)	R_s (Ω cm^2)	R_{t1} (kΩ cm^2)	CPE_1 (μF cm^{-2})	α_1	R_{t2} (kΩ cm^2)	CPE_2 (μF cm^{-2})	α_2	W (Ω cm^2 s$^{-1/2}$)
(a)								
0.0	15.2	4.5	11.42	0.5	106.1	0.95	0.6	223.1
0.5	16.1	3.6	12.50	0.4	72.3	1.68	0.5	170.3
1.0	18.7	3.4	12.57	0.6	63.1	3.30	0.6	143.7
2.0	19.1	3.2	12.66	0.7	51.5	4.58	0.5	130.1
4.0	19.1	3.0	12.62	0.7	38.4	5.13	0.6	119.5
10.0	16.1	2.8	13.73	0.7	24.5	8.22	0.5	111.8
25.0	15.9	2.5	15.91	0.6	16.2	15.38	0.6	–
45.0	15.9	2.5	16.35	0.6	15.8	15.61	0.7	–
65.0	16.5	2.5	16.48	0.6	15.5	15.89	0.7	–
74.0	16.4	2.4	16.68	0.6	14.3	15.95	0.7	–
Time (h)	R_s (Ω cm^2)	R_{t1} (kΩ cm^2)	CPE_1 (μF cm^{-2})	α_1	R_{t2} (kΩ cm^2)	CPE_2 (μF cm^{-2})	α_2	W (Ω cm^2 s$^{-1/2}$)
(b)								
0.0	5.4	3.6	15.88	0.7	95.3	2.91	0.7	186.1
0.5	5.8	3.0	22.86	0.7	67.2	3.07	0.7	132.5
1.0	6.2	2.8	23.35	0.6	50.1	7.60	0.6	114.7
2.0	6.2	2.7	26.24	0.6	37.8	8.30	0.6	101.0
4.0	5.7	2.5	26.53	0.6	29.3	9.60	0.6	93.2
10.0	5.1	2.1	28.99	0.6	22.1	13.72	0.6	88.3

Time (h)	R_s (Ω cm^2)	R_t (kΩ cm^2)	CPE (μF cm^{-2})	α
25.0	4.9	15.4	11.60	0.8
45.0	6.3	10.8	15.50	0.8
65.0	7.5	7.5	17.30	0.7
74.0	7.3	6.1	20.10	0.7

Time (h)	R_s (Ω cm^2)	R_{t1} (kΩ cm^2)	CPE_1 (μF cm^{-2})	α_1	R_{t2} (kΩ cm^2)	CPE_2 (μF cm^{-2})	α_2
(c)							
0.0	87.5	3.2	35.10	0.8	78.5	35.09	0.5
0.5	4.4	2.6	37.40	0.7	45.4	35.28	0.6
1.0	1.7	2.1	38.95	0.7	34.0	35.36	0.6
2.0	1.7	2.0	39.40	0.6	17.6	35.39	0.5
4.0	1.5	1.9	39.73	0.8	13.1	35.48	0.5
10.0	1.2	1.4	39.96	0.8	9.7	35.64	0.5

Time (h)	R_s (Ω cm^2)	R_t (kΩ cm^2)	CPE (μF cm^{-2})	α
25.0	1.9	5.6	20.83	0.6
45.0	1.8	4.7	21.91	0.5
65.0	1.7	3.9	22.10	0.5
74.0	1.6	1.5	23.50	0.5

Time (h)	R_s (Ω cm^2)	R_t (kΩ cm^2)	CPE (μF cm^{-2})	α
(d)				
0.0	1.0	61.7	39.00	0.7
0.5	1.1	41.3	41.15	0.7
1.0	1.2	31.7	41.62	0.8
2.0	1.6	15.8	42.15	0.7

Table 3 continued

Time (h)	R_s (Ω cm^2)	R_t (kΩ cm^2)	CPE (μF cm^{-2})	α
4.0	1.6	11.9	42.63	0.7
10.0	1.6	9.9	42.93	0.8
25.0	1.7	4.5	44.63	0.8
45.0	1.6	1.8	45.05	0.7
65.0	2.4	1.3	46.48	0.6
74.0	2.4	1.1	47.69	0.6

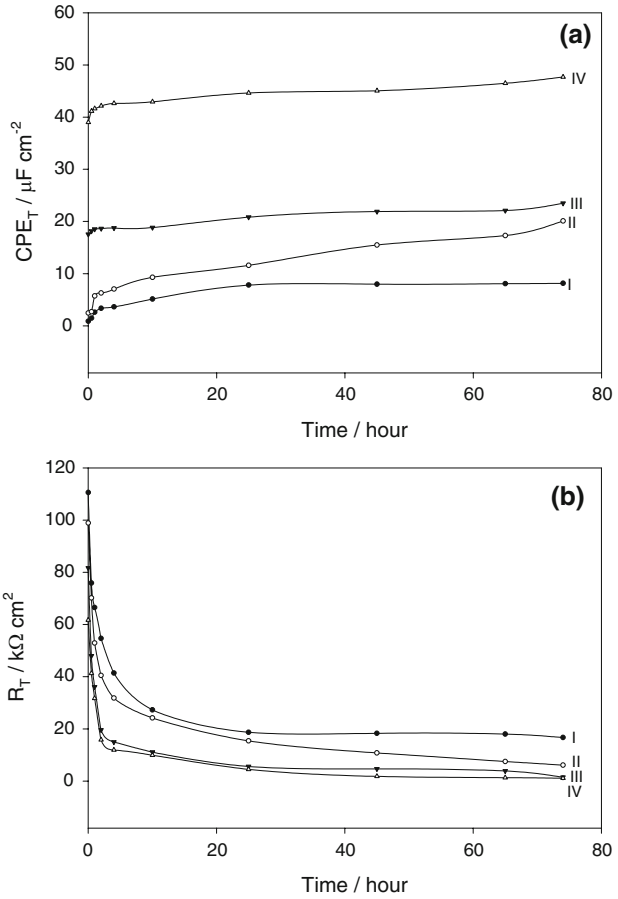

Fig. 6 Variation of total double layer capacitance (CPE_T) and total transfer resistance (R_T) value for I–IV coated electrodes with time in 3% NaCl solution at 298 K

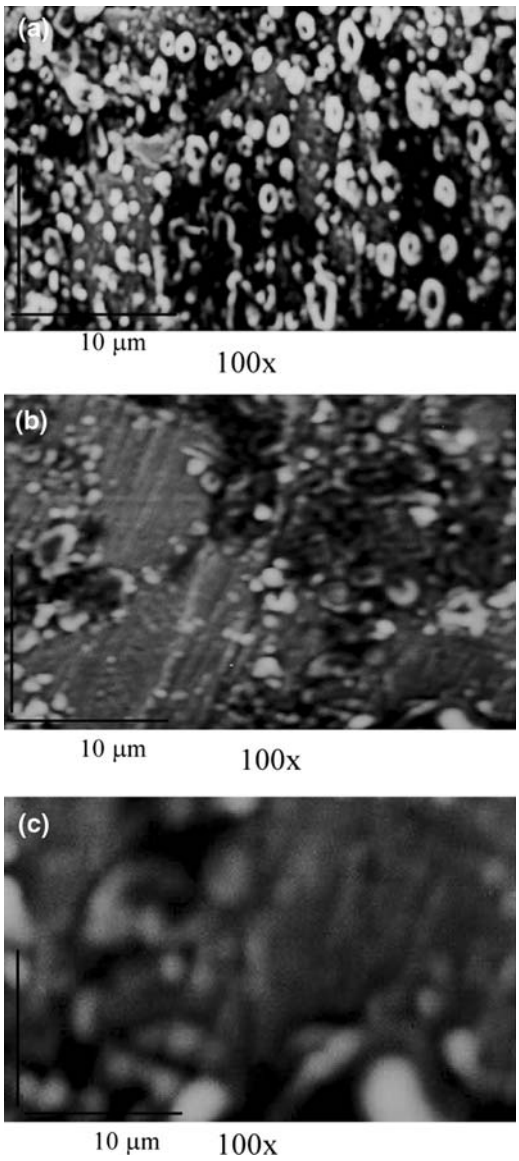

Fig. 7 SEM micrographs of **a** uncoated; and **b** coated-electrode IV; **c** coated-electrode I after immersion (74 h) in 3% NaCl solution, respectively, at 298 K

before they were examined by scanning electron microscopy (SEM). Figure 7a shows the SEM image of uncoated-mild steel after immersion in 3% NaCl solution for 74 h. It found to contain a lot number of pits due to the aggressive action of chloride ions. The visual test of the treated sample after coating with the PVS shows a transparent film on the metal surface. This film provides good protection against corrosion. After immersion in 3% NaCl solution, Fig. 7b represents as an example the SEM image for coated specimen IV, shows a loose and porous corrosion product layer with pits [39]. All of these pits are due to the attack with aggressive chloride ions. However, polysilsesquioxane-coated electrode IV was shown to have higher stability and low permeability in aggressive

solution than uncoated one. So, it shows much better film properties, which seemed to provide some corrosion protection to the metal beneath them by restricting the mass transfer of reactants and products between the bulk solution and the metal surface. Figure 7c shows the SEM image of coated electrode I where the number of pits is much lower than electrode IV. It could be seen that PVS-coated electrode I has the highest anticorrosion property. As a result, the reduction of cumulative mass loss with polymer concentration could be explained by surface morphology characters of the corrosion product scale [40].

4 Conclusion

1 PVS-coated steel electrodes (I–IV) were investigated in 3% NaCl solution at 298 K using various electrochemical techniques. The results of polarization measurements showed that corrosion current density (i_{corr}) decreases in the order IV > III > II > I.
2 The film resistance and its relative thickness increase from coated electrode IV to I as evaluated from EIS measurements.
3 OCP, EIS, and polarization results are in good agreement with each other. The obtained results were confirmed by surface examination using scanning electron microscope.

References

1. Prevost V, Petit A, Pla F (1999) Synth Met 104:79
2. Özdemir C, Can HK, Çolak N, Güner A (2006) J Appl Polym Sci 99:2182
3. Jeevananda T, Siddaramaiah S, Seetharamu S, Saravanan S, D'Souza L (2004) Synth Met 140:247
4. Chen S-M, Fa YH (2003) J Electroanal Chem 553:63
5. Borole DD, Kapadi UR, Mahulikar PP, Hundivale DG (2006) Mater Lett 60:2447
6. Herrasti P, Recio FJ, Ocon P, Fatas E (2005) Prog Org Coat 54:285
7. Rahman SU, Abul-Hamaley MA, Abul Alem BJ (2005) Surf Coat Technol 200:2948
8. Tuken T, Yazıcı B, Erbil M (2007) Mater Des 28:208
9. Tuken T, Tansuğ G, Yazıcı B, Erbil M (2007) Prog Org Coat 59:88
10. Baney RH, Itoh M, Sakakibara A, Suzuki T (1995) Chem Rev 95:1409
11. Abe Y, Gunji T (2004) Prog Polym Sci 29:149
12. Orgaza F, Rawsonb H (1986) J Non-Cryst Solids 82:378
13. Takamura N, Taguchi K, Gunji T, Abe Y (1999) J Sol–Gel Sci Technol 16:227
14. Abe Y, Kagayama K, Takamura N, Gunji T, Yoshihara T, Takahashi NJ (2000) Non-Cryst Solids 261:39
15. Liu WC, Yu YY, Chen WC (2004) J Appl Polym Sci 91:2653
16. Takamura N, Gunji T, Hatano H, Abe Y (1998) J Polym Sci Polym Chem 37:1017
17. Abe Y, Taguchi K, Hatano H, Gunji T, Nagao Y, Misono T (1994) J Sol–Gel Sci Technol 2:131
18. Abe Y, Namiki T, Tsuchida K, Nagao Y, Misono TJ (1992) Non-Cryst Solids 147:47
19. Yağan A, Pekmez NÖ, Yıldız A (2008) Electrochim Acta 53:2474
20. Ameer MA, Fekry AM, El-Taib Heakal F (2004) Electrochim Acta 50:43
21. Ameer MA, Ghoneim AA, Fekry AM, El-Taib Heakal F (2006) Mat-wiss u Werkstofftech 37:589
22. Ismail KM, El-Moneim AA, Badawy WA (2001) J Electrochem Soc 148:C81
23. Fekry AM (2009) Electrochim Acta 54:3480
24. Maranhao SLA, Guedes IC, Anaissi FJ, Toma HE, Aoki IV (2006) Electrochim Acta 52:519
25. de Assis SL, Wolynec S, Costa I (2006) Electrochim Acta 51:1815
26. El-Taib Heakal F, Fekry AM, Ghoneim AA (2008) Corros Sci 50:1618
27. El-Taib Heakal F, Fekry AM, Fatayerji MZ (2009) Electrochim Acta 54:1545
28. Retter U, Widmann A, Siegler K, Kahlert H (2003) J Electroanal Chem 546:87
29. Sánchez M, Gregori J, Alonso MC, García-Jareño JJ, Vicente F (2006) Electrochim Acta 52:47
30. Macdonald JR (1987) In: Impedance spectroscopy emphasizing solid materials and systems. Wiley, New York
31. Patrito EM, Macagno VA (1994) J Electroanal Chem 375:203
32. El-Taib Heakal F, Ameer MA, El-Aziz A, Fekry AM (2004) Mat-wiss u Werkstofftech 35:407
33. Hepel M, Tomkiewicz M (1985) J Electrochem Soc 132:32
34. Kapusta SD, Hackerman N (1982) J Electrochem Soc 129:1886
35. Mansfeld F, Jeanjaquet SL, Kendig MW (1986) Corros Sci 26:735
36. Mansfeld F (1993) Electrochim Acta 38:1891
37. Sekine I (1997) Prog Org Coat 31:73
38. Xing Wentao, You Bo, Wu Limin (2008) J Coat Technol Res 5:65
39. Vignal V, Krawiec H, Heintz O, Oltra R (2007) Electrochim Acta 52:4994
40. Jiang X, Zheng YG, Ke W (2005) Corros Sci 47:2636